REPORT DOCUMENTATION PAGE

1. REPORT DATE (DD-MM-YYYY)	2. REPORT TYPE	3. DATES COVERED (From - To)
31-12-2017	Performance/Technical Report (Quarterly)	10/01/2017 – 12/31/2017

4. TITLE AND SUBTITLE

A Hybrid Approach to Composite Damage and Failure Analysis Combining Synergistic Damage Mechanics and Peridynamics

5a. CONTRACT NUMBER

5b. GRANT NUMBER
N00014-16-1-2173

5c. PROGRAM ELEMENT NUMBER

6. AUTHOR(S)
Dr. Ramesh Talreja

5d. PROJECT NUMBER

5e. TASK NUMBER

5f. WORK UNIT NUMBER

7. PERFORMING ORGANIZATION NAME(S) AND ADDRESS(ES)

Texas A&M Engineering Experiment Station (TEES)
400 Harvey Mitchell Parkway, Suite 300
College Station, Texas 77845

8. PERFORMING ORGANIZATION REPORT NUMBER

M1601473 / 505170-00001/2

9. SPONSORING / MONITORING AGENCY NAME(S) AND ADDRESS(ES)
Office of Naval Research
875 N. Randolph Street, Suite 1425
Arlington, VA 22203-1995

10. SPONSOR/MONITOR'S ACRONYM(S)
ONR

11. SPONSOR/MONITOR'S REPORT NUMBER(S)

12. DISTRIBUTION / AVAILABILITY STATEMENT
unlimited

13. SUPPLEMENTARY NOTES

14. ABSTRACT

The work performed in the reporting period has been focused on completion of Tasks 1.2 and 1.3 related to Synergistic Damage Mechanics and Tasks 2.2 and 2.4 related to Peridynamics, as described in the project proposal. The activities related to Task 1.2 concern growth and instability of initiated cracks in the environment of the disordered fiber distribution, and Task 1.3 evaluates the effect of these cracks on the response of the composite to imposed impulses. The activities related to Task 2 cover the new peridynamic model for elasticity and fracture at an interface in a multi-phase composites.

15. SUBJECT TERMS
Computational micromechanics; Cavitation induced cracking; Peridynamics; Porous media

16. SECURITY CLASSIFICATION OF:			17. LIMITATION OF ABSTRACT	18. NUMBER OF PAGES	19a. NAME OF RESPONSIBLE PERSON
a. REPORT	**b. ABSTRACT**	**c. THIS PAGE**	SAR	6	William Nickerson
U	U	U			**19b. TELEPHONE NUMBER** (include area code) 703-696-8485

**A Hybrid Approach to Composite Damage and Failure Analysis
Combining Synergistic Damage Mechanics and Peridynamics**

Award Number N00014-16-1-2173

DOD – NAVY – Office of Naval Research

PI: Ramesh Talreja
Co-PI: Florin Bobaru

Executive Summary

The work performed in the reporting period has been focused on completion of Tasks 1.2 and 1.3 related to Synergistic Damage Mechanics and Tasks 2.2 and 2.4 related to Peridynamics, as described in the project proposal. The activities related to Task 1.2 concern growth and instability of initiated cracks in the environment of the disordered fiber distribution, and Task 1.3 evaluates the effect of these cracks on the response of the composite to imposed impulses. The activities related to Task 2 cover the new peridynamic model for elasticity and fracture at an interface in a multi-phase composites.

Tasks 1.2 and 1.3 Modeling of RVE based growth of matrix ply cracks

In the RVE constructed as described in previous quarterly reports, the growth of initiated cracks was studied in the reporting period. The model assembly (embedded cell model) is once again shown in Fig. 1 for easy reference.
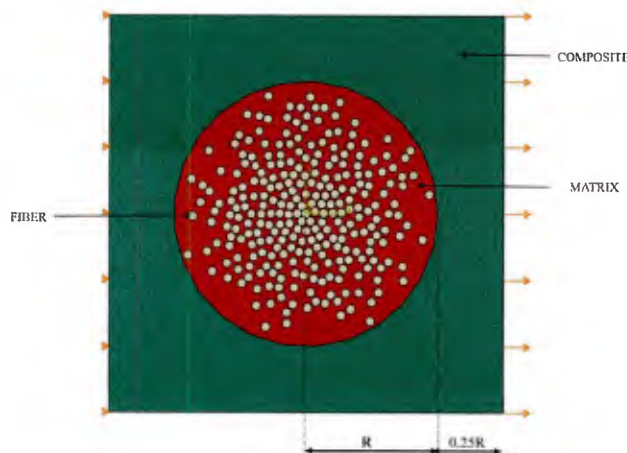

Figure 1: Model Assembly of the RVE

Using the dilatation energy density crierion for brittle cavitation, the initiation of fiber/matrix debonding was predicted in five realizations for each case of selected fiber mobility during composite processing. Loading of the model was continued until two, four or six adjacent debond cracks were found to form. In each of those RVE realizations, the debonded fibers were replaced by a crack normal to the applied tension load. For each of these transverse crack cases, the strain energy release rate was calculated via the J-integral. The path chosen for the J-integral was entirely in the matrix without enclosing any fiber, assuring that the driving force for the transverse crack was for growth in the matrix. The path independency of the J-integral was checked for each calculation. The objective of these calculation was to find the "real" crack driving force and compare it to the "assumed" driving force based on homogenization of the composite.
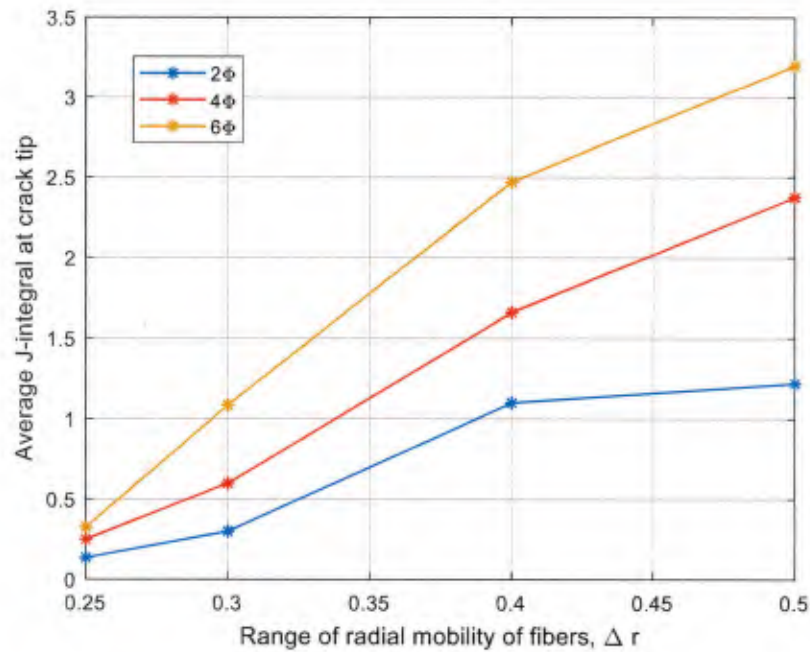

Figure 2: J-integral averaged over five RVE realization for initial transverse crack formed by coalescence of 2, 4 or 6 fibers.

Figure 2 plots the J-integral averaged over five RVE realizations for three cases of initial crack formation, namely, by coalescence of two, four or six adjacent fiber/matrix debonds. The crack driving force (J-integral) is shown at different increasing values of fiber mobility, i.e., the range of maximum random radial displacement a fiber is given in simulation of the manufacturing process. As seen in the figure, the crack driving force increases initially at a high rate and then less so, to approach a constant value at high fiber mobility. This is consistent with the fact that in the limiting case when fibers are very far apart, the crack grows in the matrix at the driving force it would have in the matrix alone without fibers. Since the J-integral for a homogeneous isotropic elastic solid is proportional to the crack size, the approaching constant value will also be in proportion to the crack size, as suggested by the curves in Fig. 2.

Figure 3 plots the ratio of the crack driving force in the "real", i.e., as-manufactured composite to the one calculated by assuming the composite to be a homogeneous orthotropic solid, as commonly assumed. The ratio $K = J_{real}/J_{homog}$, where J_{real} is as shown in Fig. 2, averaged over five RVE realizations, shows increasing differences between the real and assumed values as the fiber mobility during the manufacturing process increases. It is to be noted that the fracture toughness, i.e., the resistance to crack growth in the case of J_{real} is the matrix fracture toughness, while it is the composite fracture toughness for a UD composite with a transverse crack.
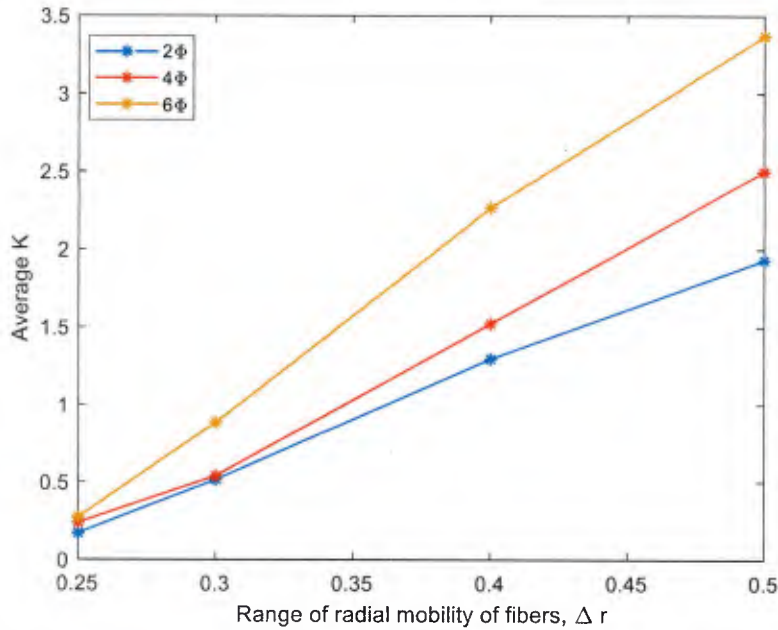

Figure 3: The ratio $K = J_{real}/J_{homog}$ is plotted against the range of fiber mobility during processing.

The ongoing research will incorporate voids along with irregular fiber distributions as consequences of composite manufacturing. The crack opening displacement in the as-manufactured composite will also be studied in conjunction with the SDM analysis.

Tasks 2.2 and 2.4 Modeling of material interfaces and damage initiation and failure in a two-phase composite material.

In a two-phase material PD model, three types of bonds exist:
- Bonds with both ends in phase-I
- Bonds with both ends in phase-II
- Interface bonds with one end in phase-I and the other in phase-II.

We can also encounter a fourth type: bonds that have their ends in a single phase, but cross the other phase (see Figure 4). This happens when the horizon size is large, relative to the size of inclusions. As the horizon is decreased below the size of inclusions, such bonds should not exist. A convergence study in terms of horizon size is expected to show differences between cases when the fourth kind of bonds are still present, and cases when

the horizon is sufficiently small and no bonds of the fourth kind are present. For a heterogeneous material, unique properties should be selected for interface bonds. In Fig. 4, the schematic for a discretized version of a peridynamic model near a material interface is shown. The uniform grid used to discretize the domain convenient. The estimation of micromodulus for an interface bond connecting nodes from two dissimilar materials has been of concern to numerous researchers. Some authors have used the harmonic or the arithmetic average of bond constants. However, considering the harmonic or arithmetic average for the interface bond gives only one value for all interface bonds, and does not take into account how much of each bond is contained on one of the phases. In order to compute the mechanical behavior at an interface more accurately, one should consider this aspect into the model. Notice also that for interfaces with non-uniform geometries, determining the bond-split between the two phases is difficult. Here, we introduce a *new method* to approximate the interface bond length included in each phase. We then determine the interface bond micromodulus by using the harmonic average of two area-adjusted micromoduli corresponding to each side of the bond. The adjusted areas (volumes in 3D) are estimated based on how much of the horizon region of each of the bonds' end-points is contained in each of the material phases. Thus, the area-adjusted micromoduli for the two portions of the interface bond are defined as:

$$c_{x\_adj} = \frac{c_x A_{1x} + c_{\hat{x}} A_{2x}}{A_x} \ , c_{\hat{x}\_adj} = \frac{c_x A_{1\hat{x}} + c_{\hat{x}} A_{2\hat{x}}}{A_{\hat{x}}}$$

where c_{x_adj} and c_x are the area-adjusted micromodulus, and the micromodulus for bonds in the phase where node x lies; A_{1x} and A_{2x} are the summation of nodal areas within the horizon of point x belonging to phases 1 and 2, respectively. Similarly, for point $\hat{x}$.
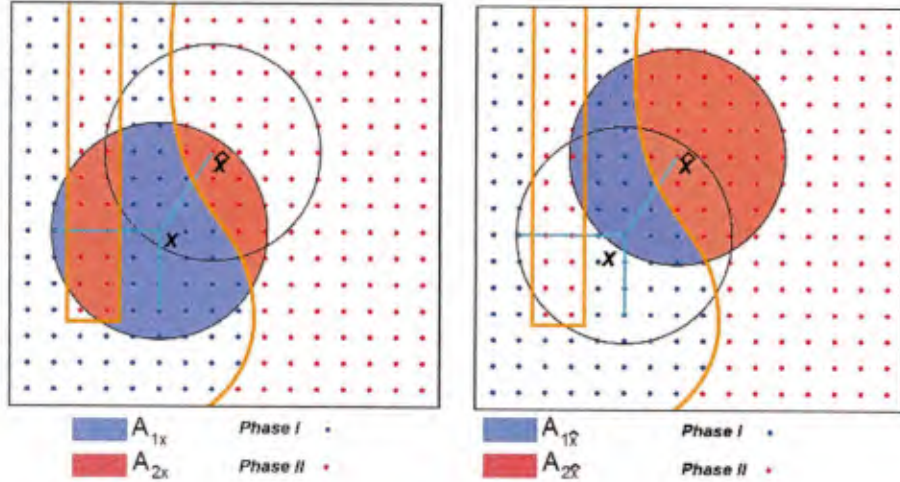

Figure 4: The area-averaging scheme for computing bond properties for interface bonds connecting one phase to the other. For convergence of response, the PD horizon size needs to be smaller than the smallest dimension of the microstructural features

Finally, the interface bond micromodulus is defined based on the harmonic average between c_{x_adj} and $c_{\hat{x}\_adj}$ as:

$$c_{int} = \left(\frac{c_{x\_adj}^{-1} + c_{\hat{x}\_adj}^{-1}}{2}\right)^{-1}$$

The areas A_{1x}, A_{2x}, $A_{1\hat{x}}$ and, $A_{2\hat{x}}$ are shown in Fig. 4. The equations above are consistent with finding bond properties for bonds in a single phase as well.

To validate the proposed approach in calculating the elasticity of composite materials, we perform a simple tension test on a bi-material model with the Young moduli of the two phases as 91 GPa and 21.9 GPa, respectively. The sample size is 100 mm × 50 mm and is subjected to the tensile stress of 1MPa applied via the fictitious node method. We perform a δ-convergence study with the horizon factor of 5 in PD and compare strain in the loading direction with a FEM solution (of the classical model) from ANSYS. Plane181 element with plane stress assumption is used in the FE model. The left edge is constrained in x direction and the opposite edge is subjected to 1MPa pressure (ANSYS does not allow the, mathematically equivalent, tensile stresses applied at both ends without any displacement constraints).

Horizontal strains along the center line crossing the material interface are shown in Fig. 5. In this figure, we show the δ–convergence results for the area-adjusted harmonic average method. In the limit of the horizon becoming small, the PD results become indistinguishable from the FEM results (obtained here with ANSYS). These results are for the three approaches to computing properties of interface bonds. We show these results for one of the larger horizons to be able to see the differences from the classical result a little easier. Note the oscillations from the earlier PD models that were using arithmetic or harmonic averaging methods.
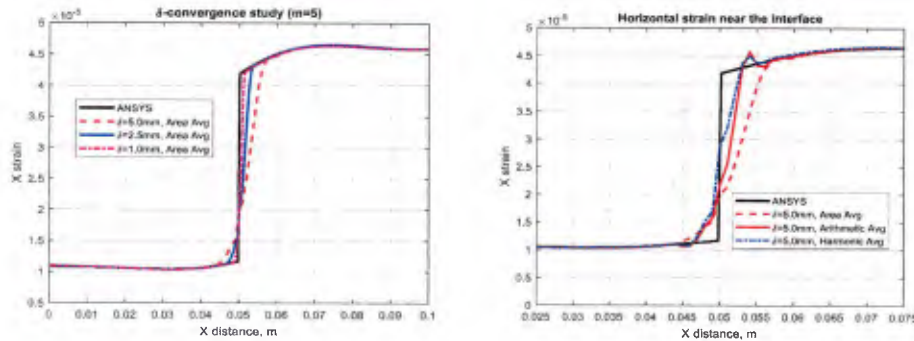

Figure 5: Left: Nodal horizontal strains along the bi-material sample centerline from the FEM, and the PD with different horizon values (using area averaging and fictitious nodes); Right: Horizontal strains for the "large horizon" case, near the interface obtained from different PD models for material interfaces: area, arithmetic, and harmonic averaging methods.

We test the model for the drop-test of a solder joint composed of a matrix material with intermetallic inclusions (Fig. 6). The results confirm experimental observations (see [1])

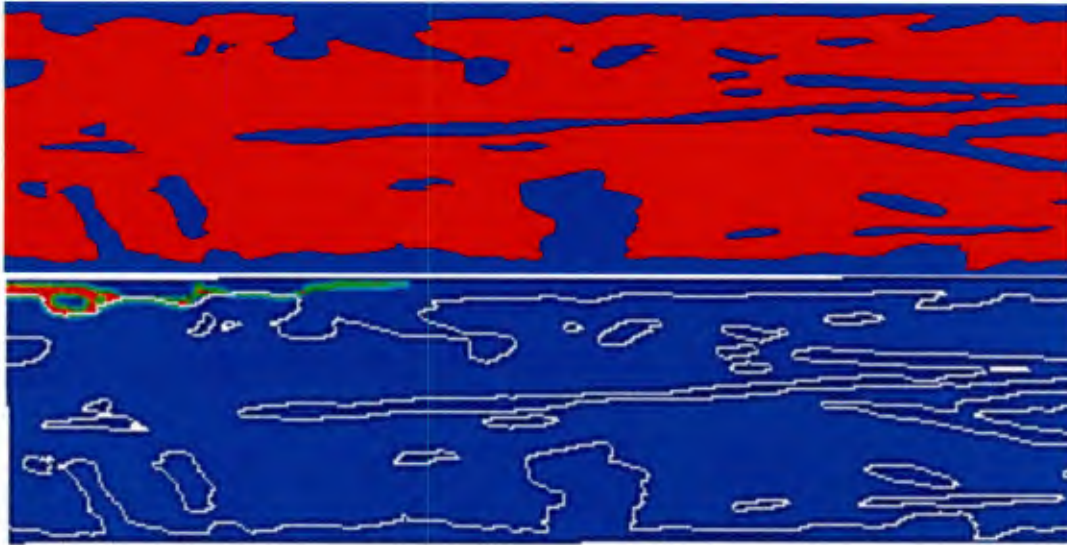that cracks propagate along the interface between the matrix and the inclusions, and though the inclusions.

Figure 6: Top: microstructure of the solder join: red color is the matrix material, blue color are the inclusions. Bottom: Damage index map at 1ms after impact for the sample with large inclusions, plotted over the solder joint microstructure contours.

References:
[1] Javad Mehrmashhadi, Yuye Tang, Xiaoliang Zhao, Zhanping Xu, Jianbiao Pan, Quang Van Le, Florin Bobaru (2017),"The Effect of Solder Joint Microstructure on the Drop Test Failure: a Peridynamic Analysis", under review.